Progress In Electromagnetics Research C, Vol. 20, 95–109, 2011

A CIRCULARLY POLARIZED APERTURE STACKED PATCH MICROSTRIP ANTENNA FOR L BAND

F. Zhao

College of Electronic Science and Engineering
National University of Defense Technology
47 Yanwachi Street, Changsha 410073, China

T. T. Liu and Z. P. Qian

Institute of Communications Engineering
PLA University of Science and Technology
Yudao Street, Nanjing 210007, China

Abstract—The design and manufacture of a circular polarized aperture stacked patch circular microstrip patch antenna (CPASPA) at L-band is presented. The Wilkinson power divider is used to excite the stacked circular patches by two orthogonal H-shape slots, which can improve the operation bandwidth and circularly polarized performance. The design is optimized by a series of parametric study of the input impedance for the antenna. The measurements show that the CPASPA has a 3-dB axial ratio (AR) bandwidth of 55.0% and a 10-dB return loss (RL) bandwidth of 47.0%. The measured gain is more than 0 dBic over the bandwidth of 42.5%, in which the maximum is 9.4 dBic. The measurements agree very well with the simulation results.

1. INTRODUCTION

Recent years have seen a tremendous growth in demand for wide-band telecommunications services in the L-band frequencies in areas such as mobile satellite, terrestrial cellular, and personal communications systems. And the circular polarized (CP) antennas play a vital role in obtaining the communication link between a base station and a mobile unit [1, 2]. Microstrip antennas offer many attractive features such as low profile, light weight, easy fabrication, integrability with microwave

Received 27 November 2010, Accepted 9 February 2011, Scheduled 3 March 2011
Corresponding author: Fei Zhao (feizhao1983@hotmail.com).

and millimeter-wave integrated circuits, and conformability to curved surfaces [3, 4]. Besides, the CP microstrip antennas have been developed with both single [5–9] and dual [10–12] feed arrangement. For the single feed case, some modifications including trimming the corners of a square patch, feeding the patch at adjacent sides, and cutting a slot inside the patch, are used to fulfill the CP condition. However, it is difficult to obtain the wide-band characters especially in impedance, gain, and AR. Such as the antenna reported in [5] yields an AR bandwidth (AR ≤ 3 dB) of 0.6% and the impedance bandwidth (RL ≤ -10 dB) of 2.3%, the antenna in [6] attains the impedance bandwidth of 0.03% and the AR bandwidth of 1.1%. Nasimuddin and Verma [7] have used two stacked rectangular patches and the foam layer to design wide-band single feed CP antenna. By optimizing the feed location and foam thickness, it achieves the 10-dB RL bandwidth of 21.0% and 3-dB AR bandwidth of 13.5%. Yang et al. [8] adopt a U-slot patch and/or L-probe to improve the impedance bandwidth effectively. The antenna attains the 10-dB RL bandwidth of 37.0%, but 3-dB AR bandwidth of merely 7.6%. Although the thick substrate is used, the 3-dB AR bandwidth is less than 17% with the RL bandwidth decreased to 25.3%. Kasabegoudar and Vinoy [9] posed the CP microstrip antenna on a suspended substrate with a coplanar capacitive feed and a slot within the rectangular patch. The antenna achieves the 3-dB AR bandwidth of only 7.1%.

Adopting dual feed could easily excite two orthogonal field components with equal amplitude but a 90° phase difference. It could get wider AR bandwidth due to the insensitivity to frequency [3, 4, 10–12]. And the most elegant configuration for impedance bandwidth enhancement is an aperture (slot)-coupled microstrip patch antenna proposed by Pozar in [13]. The single circular patch antenna fed by two rectangle coupling slots is proposed by Karmakar and Bialkowski [10]. The minimum AR in its operation bandwidth is 0.6 dB, and the 3-dB AR bandwidth is more than 20%. Notwithstanding, the location and shape of slots are not optimized, which results in low front-to-back ratio. In [11], the C-shape and rectangle coupling slots are used to feed the single patch antenna, yielding 10-dB RL bandwidth of about 20.0% and 3-dB axial ratio bandwidth of more than 30%. However, the worst-case front-to-back ratio of its co-polar radiation patterns approximates 10 dB in its operation bandwidth.

The design of the L band dual feed CPASPA is presented in the next section. The coupled slots are in H shape, which is proved for the maximum coupling and minimum backward radiation by the experiments in [14]. Meanwhile, the slots are symmetrically oriented about the diameter of the patch, conjoined by the Wilkinson power

divider for CP radiation. Moreover, two stacked patch structure [7] is used to improve the impedance bandwidth simultaneously, which is not used in [10, 11]. The aperture coupling stacked patch (ASP) antennas are also introduced in [15–17], but they are all single linear polarize antennas, and the stacked patches are rectangular. In addition, the adjustable air layer and the "screw-support" structure [18] adopted in manufacture ensure stable antenna performance. Details of the antenna design and experimental results of the excellent performance of antenna are presented and discussed. The presented design can easily be extended to other band satellite and terrestrial systems that require circularly polarized antennas operating over a similar bandwidth.

2. ANTENNA CONFIGURATION AND DESIGN PROCEDURE

The geometry of CPASPA is shown in Figure 1. The antenna consists of three dielectric substrate layers and an air layer. The circular patches are adopted, which could obtain better CP performance and wider bandwidth than rectangle patches. The parasitic circular patch of radius r_1 is etched on the parasitic patch substrate with thickness h_1 and dielectric constant ε_{r1}. Notice that the patch is inversed, so the substrate acts as the radome for environmental protection. The driven circular patch having a radius of r_2 is etched on the driven patch substrate with thickness h_2 and dielectric constant ε_{r2}. In order to increase the operational bandwidth furthermore, the distance between two patches is increased by sandwiching an air layer of thickness h_0. The driven patch is fed from two orthogonal symmetry H-slots defined

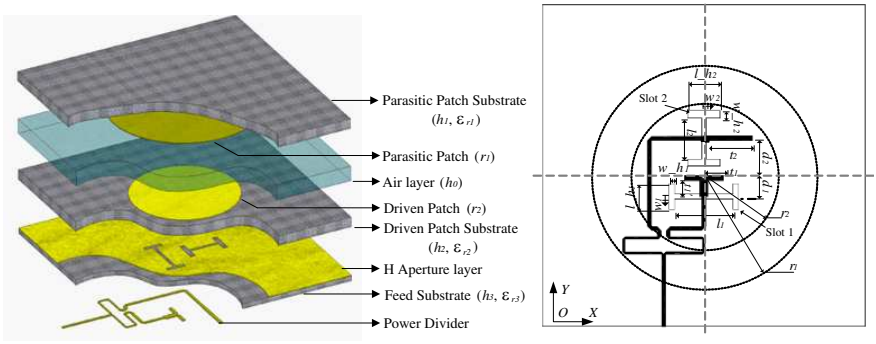

Figure 1. Geometry of the CPASP. (a) Configuration of the CPASPA antenna. (b) Top view of the CPASPA geometries

by parameters l_1, w_1, l_h_1, w_h_1, l_2, w_2, l_h_2, and w_h_2 which are shown in Figure 1(b). Slot 1 is along X direction, whose offset from the origin in direction Y is d_1. But in contrast, slot 2 is along Ydirection, whose offset from the origin is d_2. This arrangement for the 2 slots could enhance the isolation between the two orthogonal aperture fields on two patches [18]. The H-slot layer is etched on feed substrate with thickness h_3 and dielectric constant ε_{r3}. While the Wilkinson power divider is etched on the bottom of this substrate, and the time delay microstrip line is used to obtain 90° phase shift in X direction. In order to obtain a suitable impedance match for both two ports of the power divider, two open-circuited stubs of lengths t_1', t_1 and t_2 is used as shown in Figure 1(b). Note that the form of two stubs differs due to the confine of the area for feed substrate.

With the presence of the orthogonal aperture coupling feed structure, the AR-bandwidth and quality of CP are improved obviously due to the high isolation between the orthogonal TM_{11} fields on both patches [18]. And the bandwidth enhancement techniques use a common trait of the wide-band characteristics resulting from coupled resonances. The operation of this configuration makes the two coupled resonances: the lower frequency resonance is over coupled to the microstrip feed line, and the higher one is a low Q resonance between the two patches [15].

Based on the operation principle of the CPASPA described above, the parameters for three substrates follow these rules: the thickness and dielectric constant of driven and parasitic substrate affect the impedance and polarize bandwidth; the thicker and lower dielectric constant make the wider impedance due to the lower Q value, but a too thick substrate tends to excite the surface and high order mode wave on the patch, which may bring on the deterioration of CP performance. On the contrary, a thinner and higher dielectric constant feed substrate profits the driven patch to couple electromagnetic energy (EM) form the feed net and to decrease the backward radiation. In this design, $\varepsilon_{r1} = \varepsilon_{r2} = \varepsilon_{r3} = 2.55$, $h_1 = 0.5\,\text{mm}$, $h_2 = h_3 = 1.5\,\text{mm}$.

Then, some critical initial geometry values are chosen as follows: The initial r_2 is obtained by using well-known design Equations (1) (2) [3]:

$$r = \frac{c\chi'_{11}}{2\pi f_{11}\sqrt{\varepsilon_r}} \tag{1}$$

$$r = r'\left[1 + \frac{2h}{\pi a'\varepsilon_r}\left(\ln\frac{\pi a'}{2h} + 1.7726\right)\right]^{0.5} \tag{2}$$

where c is the speed of light in free space; χ_{11} is the first zero for the derivative of the Bessel function; f_{11} is the operation frequency

of the circular microstrip antenna; h is the thickness of the driven substrate; lastly, r and r' are the effective radius and physics radius of the patch, respectively. The initial radius of the parasitic patch $r_1 = (1.2 \sim 1.4) \times r_2$, the initial thickness of the air layer $h_0 = (0.05 \sim 0.09) \times \lambda_0$, at the last, the width and length of the both slots are defined by $\lambda_0/(8 \sim 10)$ and $\lambda_0/(60 \sim 80)$ respectively [10].

3. PARAMETRIC STUDY

To achieve optimum performance, a parametric study by using simulation software CST Microwave Studio is carried out to investigate the characteristics of the proposed CPASPA. The final geometry values of the optimized antenna are shown in Table 1.

Table 1. The initial geometry values for CPASPA (mm).

r_1	d_1	l_1	w_1	l_h_1	w_h_1	t_1	t'_1
23.0	9.6	18.0	1.5	8	1.8	5.0	6.0
r_2	d_2	l_2	w_2	l_h_2	w_h_2	t_2	h_0
32.5	8.5	12.8	1.8	10	2.2	15.0	9.7

The parameters effects of r_1 and r_2 are similar to the effects of the edge lengths for the rectangular stacked patches which have been studied in [15, 16]. Adjusting r_1 and r_2 can control the quantity of the coupled EM between two circular patches, thereby it is used to balance the two resonances of the CPASP.

Figure 2 shows the normalized (to 50) input resistance of the antenna as a function of h_0 for both slot ports. The character of two resonances is clearly observed, due to the use of stacked patches. It brings a smaller range of impedance variation between the two resonances. Thus, a wide-band impedance match can be obtained. For brevity, the resonant frequencies and normalized resonant resistances are denoted by f_{01} and R_{01} for the lower resonance, f_{02} and R_{02} for the upper resonance, respectively. For slot 1 port, f_{01} is increased by 0.4%, while f_{02} is decreased by 3.4%, and for slot 2 port, f_{01} is increased by 0.5%, while f_{02} is decreased by 3.1%, when h_0 is increased by 25%. It is noted that the air thickness of h_0 has more effect on the higher resonance f_{02} for both slot ports. Comprehensibility, the resonance frequency for the two patches resonance structure is decreased when its volume is expanded, which is insensitive to f_{01}. Therefore, the space between two resonance frequencies can be modified flexibly, by changing h_0. This result is very useful to optimize the bandwidth

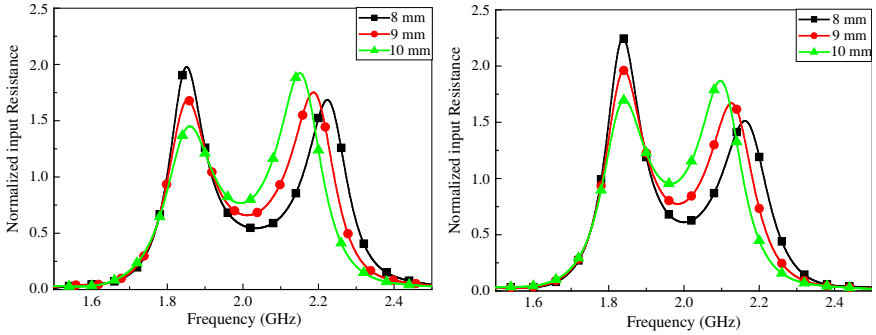

Figure 2. Normalized input Resistance as a function of h_0 for two slots ports. Other dimensions are the same as for Table 1.

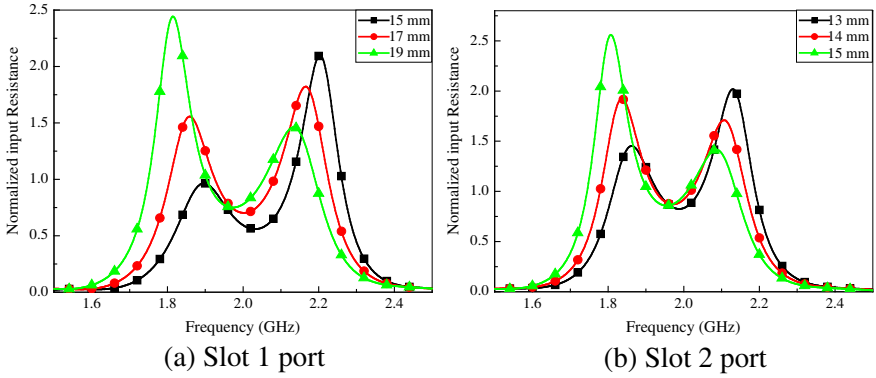

Figure 3. Normalized input Resistance as a function of l_1 and l_2. Other dimensions are the same as for Table 1.

characteristic of the antenna.

Figure 3 gives the input resistance of the antenna as a function of l_1 and l_2 for both slot ports. For slot 1 port, f_{01} and f_{02} are decreased by 4.3% and 3.2%, meanwhile R_{01} is increased by 153.1%, and R_{02} is decreased by 30.3%, when l_1 increased by 26.7%. For slot 2 port, f_{01} and f_{02} are decreased by 2.9% and 2.1%, meanwhile R_{01} is increased by 76.0%, and R_{02} is decreased by 29.9% as l_1 increased by 15.4%. Similar variation trends are shown for both the slot ports. Extending the length of slots could decrease the two resonant frequencies, especially for the lower one which is formed by the slots and driven patch. R_{01} being increased illustrates that the EM coupled form the feed line is enhanced due to the area of the slots being expanded. So the

upper resistance is weakened to hold the sum of feed energy. From the curves plotted in Figure 3, it is shown that smaller slot will bring under coupling for lower resonance, which induces R_{02} too large to lost match. However, a too large slot will make the lower resonance overcoupled, which results in a non-matching of the impedance nearby the lower resonance due to the large R_{01}. The parameters l_h_1 and l_h_2 have similar effects on the input impedance for the same principle.

The normalized input resistance as a function of d_1 and d_2 is shown in Figure 4. It is interesting to note that the variation trends of input resistance for two slot ports are no longer shown similar characters as before. For slot 1, f_{01} and f_{02} are increased by 2.3% and 2.3%, meanwhile R_{01} is decreased by 33.1%, and R_{02} is increased by 54.3%, when l_1 increased by 26.7%. However, the variety of d_2 has nearly no effects on its input resistance. The phenomena can be explained by Figure 5, which shows the two simulated surface currents distribution on the driven patch as two slot ports excited independently. For the case in Figure 5(a), the simulated surface currents along Y direction (polarization direction) are sinusoidal distribution and uniform along X direction. While in Figure 5(b), the surface currents along Y direction are uniform and sinusoidal distribution along X direction (polarization direction). Consequently, increasing d_1 along Y direction for slot 1 weakens the EM coupled form this slot, which is equivalent to shrinking the area of slot 1. This phenomenon has been described in Figure 3(a). While increasing d_2 for slot 2, the EM coupled form slot 2 is nearly constant due to the surface currents' uniform distribution.

Figure 6 shows the effects of t_2 on the input impedance for slot 2 port. From the results, the variety of the t_2 has nearly no effects on the input resistance, yet the input reactance is increased slightly as

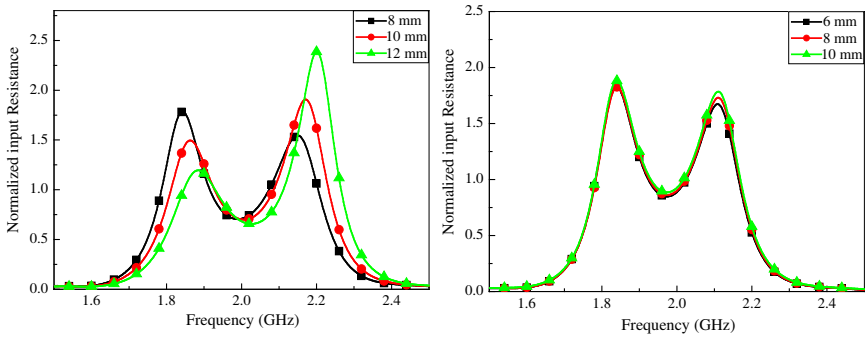

(a) Slot 1 port (b) Slot 2 port

Figure 4. Normalized input resistance as a function of d_1 and d_2. Other dimensions are the same as for Table 1.

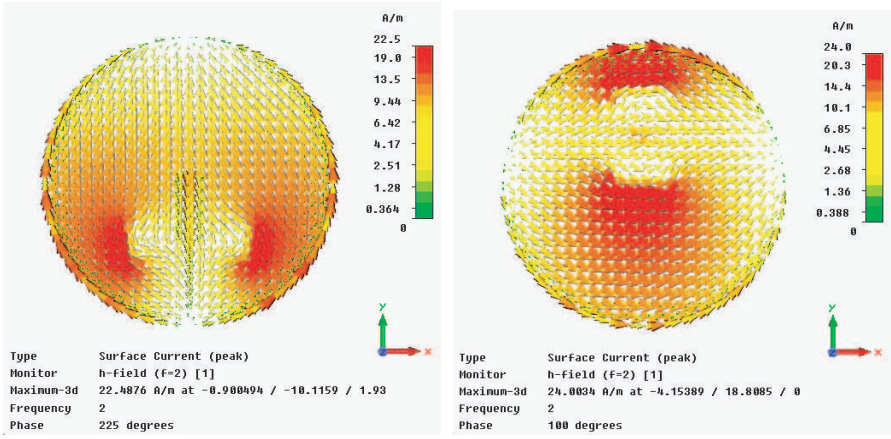

(a) Slot 1 port excited (b) Slot 2 port excited

Figure 5. The simulated surface currents distribution on the driven patch.

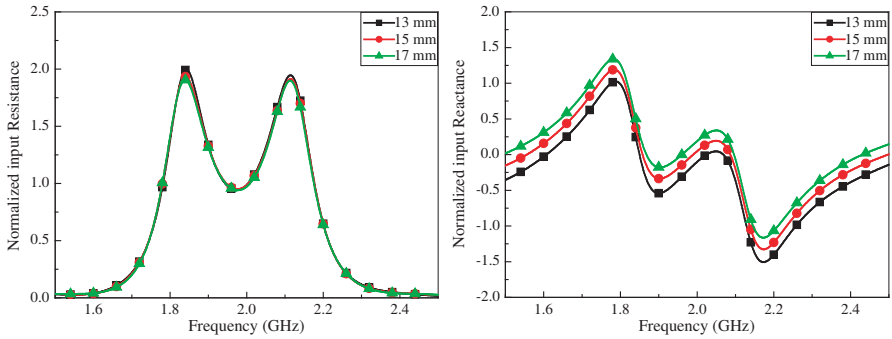

(a) Normalized input Resistance (b) Normalized input Reactance

Figure 6. Normalized input Impedance as a function of t_2 for slot 2 port. Other dimensions are the same as for Table 1.

t_2 extended. Therefore, the open-circuited stubs can be equivalent to an inductance functionally, which are used to obtain impedance match as introduced in Section 2. The parameters t_1 and t_1' have the same effects as t_2.

Figure 7 shows the variation of the isolation with frequency for different distances d between the two slot ports. A good isolation more than 45 dB is seen with the proposed antenna configuration, which

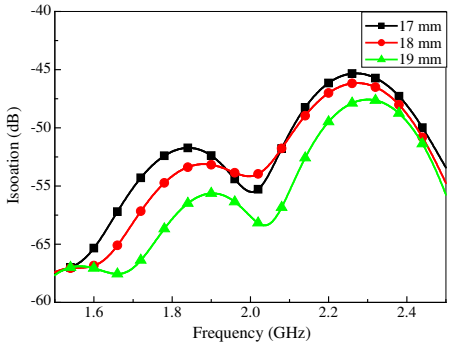

Figure 7. Isolation as a function of distance $d(d_1 + d_2)$ between two slot ports. Other dimensions are the same as for Table 1.

ensures the high CP performance. And as expected, the isolation is improved as the distance increased.

Based on the above parametric study, the design of the CPASCP could start with optimizing the impedance bandwidth for slot 1 port. Make sure that the d_1 is big enough to benefit ports isolation, on condition that the two balanced resonances are attained nearby the centre frequency. Subsequently, the impedance bandwidth for slot 2 port can be achieved by mainly adjusting the parameters of slot 2. Finally, the two slot ports are conjoined by the power divider and time delay line, with CP radiation realized. This proposed design processing could be applied to analyze similar antennas, operating at different frequencies, with slight design changes.

4. EXPERIMENTAL RESULTS AND DISCUSSION

According to the specifications given above, an antenna prototype for left hand rotation circular polarization (LHCP) was manufactured, measured and compared with simulated results. The structure of the screw-support [18] is used in fabrication. Turning the nuts on the support screws can adjust the thickness of the air layer between parasitic patch and driven patch. So it can optimize the impedance bandwidth of the CPASPA after manufacture. The horizontal location of the air layers is fixed accurately by screws, and the error of the thickness (h_0) could be easily controlled at less than 0.2 mm. According to the analysis of h_0 in Section 3, this error induces less than 0.34% variation of the two resonances. Undoubtedly, it is nearly no effect on the global performance of the antenna. The CPASPA prototype is shown in Figure 8.

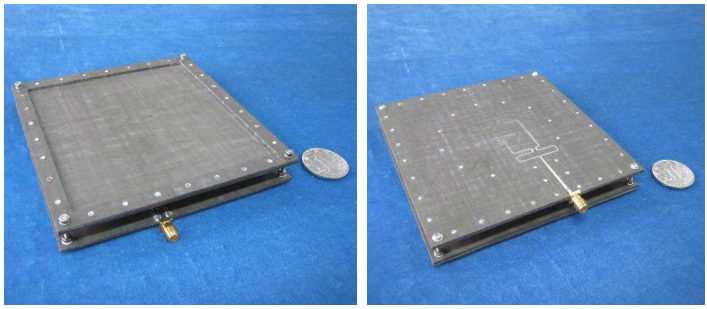

Figure 8. Photograph of CPASPA prototype.

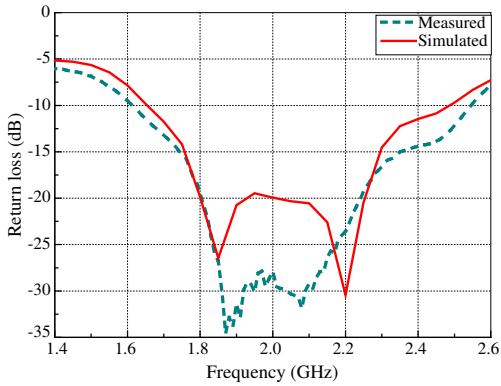

Figure 9. Measured and simulated return loss for CPASPA.

The measured and simulated return losses of the CPASPA are presented in Figure 9. The measured 10-dB return loss bandwidth is 47.0% (1.61 GHz to 2.54 GHz), and the simulated bandwidth is 41.5% (from 1.65 to 2.48 GHz). Note that the measured impedance bandwidth is wider than the simulated, and the discrepancy of the RL is larger in the vicinity of 2 GHz, because the dielectric and conductor losses are not considered in simulation, and the ohmic loss for chip-resistor of the power divider near the centre frequency is not calculated sufficiently else.

The measured and theoretical patterns for co-polarization (LHCP) and cross polarization (RHCP) at 1.7, 2.0, and 2.3 GHz in XOY planes ($\varphi = 0°$) are shown in Figure 10(a), (b), and (c), respectively. The measured radiation patterns agree well with the simulated ones. In all cases, the measured cross polarization levels are below -14 dB at the boresight angle, and as low as -30 dB at the centre

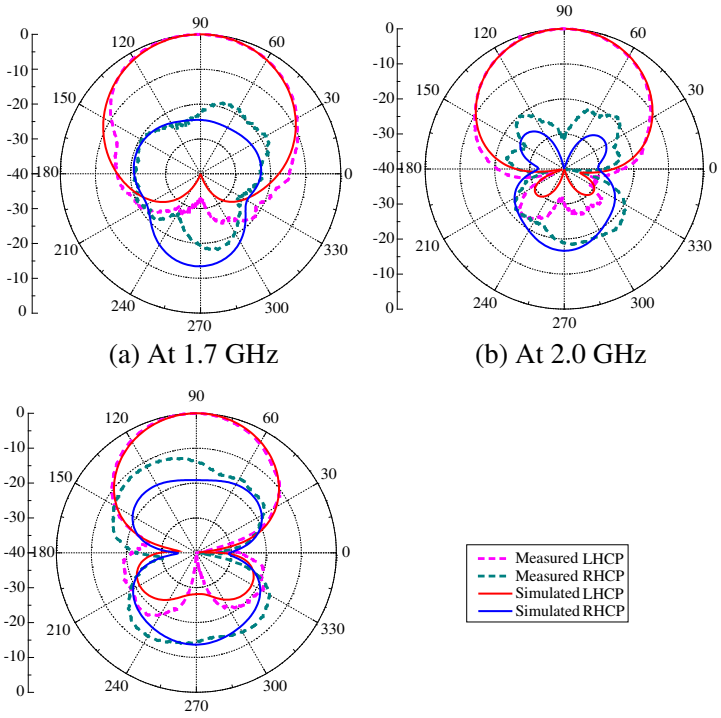

Figure 10. Measured and simulated radiation patterns for CPASPA.

frequency (2.0 GHz), which is expected because of the high-isolation feed structure. The 3 dB beam width of radiation patterns is more than 60°. Due to the H-slot, the backward radiation is reduced further. The measured worst-case front-to-back ratio of the co-polar radiation patterns is 17 dB. The back radiation can be reduced further by using a reflecting ground plane placed at a distance of $\lambda_0/4$ (λ_0 is the wavelength in free space for the centre frequency). The broad beam width and low front-to-back ratio are very useful for communications system for wide-angle coverage.

Figure 11 shows the measured gain and AR at boresight angle. Meanwhile, the corresponding simulated results are plotted in the figures for comparisons. Measurements and simulations are in good agreement. The boresight axial ratio was computed from the S_{21} data of LHCP and RHCP using Equation (3):

$$\mathrm{AR} = 20\log_{10}\left(\frac{|E_{LHCP}| + |E_{RHCP}|}{|E_{LHCP}| - |E_{RHCP}|}\right) \tag{3}$$

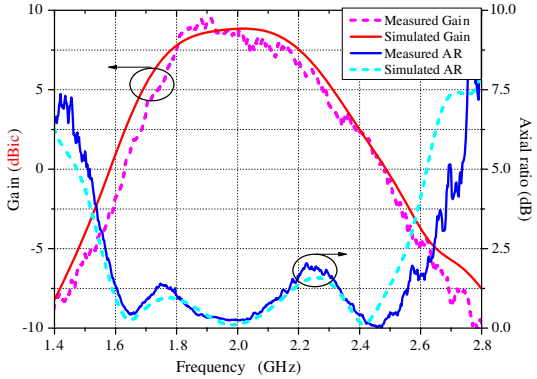

Figure 11. Measured and simulated gain and AR vs. frequency.

The measured 3-dB AR bandwidth is 55.0% (1.55 GHz to 2.65 GHz), and the simulated bandwidth is 51.5% (from 1.54 to 2.57 GHz). In addition, the minimum axial-ratio value is less than 0.3-dB at the center frequency (2.0 GHz), indicating that the circularly polarized is pure. The measured 0 dBic gain bandwidth is 42.5% (1.63 GHz to 2.48 GHz), and the simulated bandwidth is 45.5% (from 1.58 to 2.49 GHz). The measured maximum gain is 9.4 dBic at 1.91 GHz. A little shift in the bandwidth is due to the fabrication tolerances.

Note that the performance of the gain is degraded quite rapidly near the upper input impedance band edge. It is due to an increased phase difference between the currents of the two patches, which approaches 180° near the top end of the band. Figure 12 gives the surface currents on both patches in the same period (phase = 0°) at the 1.7 and 2.3 GHz. As shown in Figure 12(a), the directions of the currents on both the patches are almost the same. Contrarily, the currents at the 2.3 GHz are nearly in the opposite direction in Figure 12(b). Therefore, the patches do not radiate efficiently.

These measured results can be compared with those presented in [3] and [6–11]. Since several wide-band techniques are adopted synthetically, the CPASPA achieves more excellent bandwidth character for RL, AR and good radiation performance. Further efforts using the further thicker driven patch substrate (h_2) could effectually benefit the improvement of the bandwidth again, especially for the 3-dB gain bandwidth. Changing h_2 from 1.5 mm to 4.0 mm can enlarge the 10-dB RL bandwidth from 41.5% to 48.3% and 3-dB gain bandwidth from 29.8% to 44.3% respectively, which has been simulated and optimized on the computer. Frankly speaking, the CPASPA has excellent wide-band performance at the expense of the more complex configuration design.

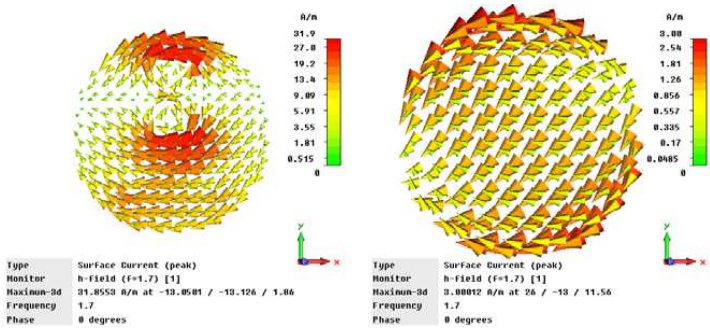

The driven patch The parasitic patch

(a) 1.7 GHz

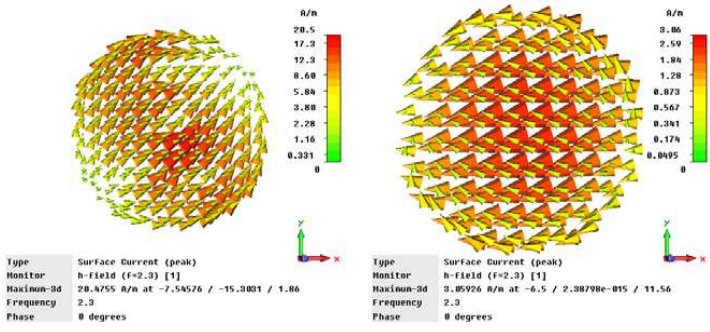

The driven patch The parasitic patch

(b) 2.3 GHz

Figure 12. The surface currents distribution on both patches.

5. CONCLUSION

The CPASPA is designed and manufactured for L band. The techniques of stacked circular patches, orthogonal H-shape slots coupled feeding, Wilkinson power divider, and "screw-support" structure are implemented to improve the operation bandwidth and performance of the prototype. The wide-band and CP performance can be optimized independently, based on the parametric study. Simulation and measurements are in good agreement. The prototype antenna shows excellent wide-band performance. Moreover, it can yield near 20% effective operation bandwidth even under rigorous requirements (AR $\leq$ 1.0 dB, RL $\leq$ 20 dB, gain $\geq$ 6.0 dB). The wide bandwidth, broad beam width, and low cross polarization make the antenna applicable for high performance wide-band communications on

aircraft. Further research will be focused on optimizing gain bandwidth and the sequential array design for the CPASPA.

ACKNOWLEDGMENT

The authors express their appreciation to Prof. Chai Shunlian, Prof. Mao Junjie and Dr. Xiao Ke of National University of Defense Technology for discussions on this work. Special thanks go to Li Hongbin of PLAUST for providing the measurements of the CPASPA.

REFERENCES

1. Wu, W. W., E. F. Miller, W. L. Pritchard, and R. L. Pickholtz, "Mobile satellite communications," *Proc. IEEE*, Vol. 82, 1431–1448, 1997.
2. Miller, B., "Satelliate free the mobile phone," *IEEE Spectrum*, Vol. 35, 26–35, 1998.
3. James, J. R., P. S. Hall, and C. Wood, *Microstrip Antenna Theory and Design*, IEE Press, Stevenage, U.K., 1981.
4. Kumar, G. and K. P. Ray, *Broadband Microstrip Antennas*, Artech House, Boston, 2003.
5. Lin, Y., H. Chen, S. Member, and S. Lin, "A new coupling mechanism for circularly polarized annular-ring patch antenna," *IEEE Transactions on Antennas and Propagation*, Vol. 56, 11–16, 2008.
6. Chen, H., Y. Wang, Y. Lin, C. Lin, and S. Pan, "Microstrip-fed circularly polarized square-ring patch antenna for GPS applications," *IEEE Transactions on Antennas and Propagation*, Vol. 57, 2009.
7. Nasimuddin, K. P. E. and A. K. Verma, "Wideband circularly polarized stacked microstrip antennas," *IEEE Antennas and Wireless Propagation Letters*, Vol. 6, 21–24, 2007.
8. Yang, S. S., K.-F. Lee, A. A. Kishk, and K.-M. Luk, "Design and study of wideband single feed circularly polarized microstrip antennas," *Progress In Electromagnetics Research*, Vol. 80, 45–61, 2008.
9. Kasabegoudar, V. G. and K. J. Vinoy, "A broadband suspended microstrip antenna for circular polarization," *Progress In Electromagnetics Research*, Vol. 90, 353–368, 2008.
10. Karmakar, N. C. and M. E. Bialkowski, "Circularly polarized aperture-coupled circular microstrip patch antennas for L-band

applications," *IEEE Transactions on Antennas and Propagation*, Vol. 5, 933–940, 1999.

11. Padhi, S. K., N. C. Karmakar, C. L. Law, and S. Aditya, "A dual polarized aperture coupled circular patch antenna using a C-shaped coupling slot," *IEEE Transactions on Antennas and Propagation*, Vol. 51, 3295–3298, 2003.
12. Vallecchi, A. and G. B. Gentili, "Design of dual-polarized series-fed microstrip arrays with low losses and high polarization purity," *IEEE Transactions on Antennas and Propagation*, Vol. 53, 2005.
13. Pozar, D. M., "Microstrip antenna aperture-coupled to a microstripline," *Electronics Letters*, Vol. 21, 49–50, 1985.
14. Rathi, V., G. Kumar, and K. P. Ray, "Improved coupling for aperture coupled microstrip antennas," *IEEE Transactions on Antennas and Propagation*, Vol. 44, 1196–1198, 1996.
15. Targonski, S. D. and R. B. Waterhouse, "Design of wide-band aperture-stacked patch microstrip antennas," *IEEE Transactions on Antennas and Propagation*, Vol. 46, 1998.
16. Gao, S., L. Li, M. Leong, and T. Yeo, "Wide-band microstrip antenna with an H-shaped coupling aperture," *IEEE Transactions on Antennas and Propagation*, Vol. 51, 2002.
17. Zhao, F., K. Xiao, W.-J. Feng, S.-L. Chai, and J.-J. Mao, "Design and manufacture of the wide-band aperture-coupled stacked microstrip antenna," *Progress In Electromagnetics Research C*, Vol. 7, 37–50, 2009.
18. Qian, Z., T. Liu, and F. Zhao, "Design of wide-band aperture-coupled circularly polarized microstrip antenna," *Chinese Journal of Radio Science*, Vol. 25, 739–744, 2010.